HAL
open science

Revisiting the relation between premixed flame brush thickness and turbulent burning velocities from Ken Bray's notes

Pascale Domingo, Luc Vervisch

To cite this version:

Pascale Domingo, Luc Vervisch. Revisiting the relation between premixed flame brush thickness and turbulent burning velocities from Ken Bray's notes. Combustion and Flame, 2021, pp.111706. 10.1016/j.combustflame.2021.111706 . hal-03372601

HAL Id: hal-03372601

https://normandie-univ.hal.science/hal-03372601v1

Submitted on 10 Oct 2021

HAL is a multi-disciplinary open access archive for the deposit and dissemination of scientific research documents, whether they are published or not. The documents may come from teaching and research institutions in France or abroad, or from public or private research centers.

L'archive ouverte pluridisciplinaire **HAL**, est destinée au dépôt et à la diffusion de documents scientifiques de niveau recherche, publiés ou non, émanant des établissements d'enseignement et de recherche français ou étrangers, des laboratoires publics ou privés.

Revisiting the relation between premixed flame brush thickness and turbulent burning velocities from Ken Bray's notes

Pascale Domingo[a], Luc Vervisch[a,*]

[a] *CORIA – CNRS, Normandie Université, INSA Rouen Normandie, 76801 Saint-Etienne-du-Rouvray, France*

Abstract

Applying the Bray-Moss-Libby (BML) bi-modal asymptotic limit to a progress variable signal in a premixed turbulent flame, a relation is established between the variation rate of the mean turbulent flame brush thickness, the flame surface wrinkling and the turbulent burning velocity. This scaling suggests that the link between the amplification of the flame surface by turbulence and the increase of the turbulent burning velocity may need to be modulated by a corrective term proportional to the rate of variation of the turbulent flame brush thickness. This correction is expected to be driven by a short relaxation time scale, which is representative of the turbulent flame brush adjusting to its continuously varying turbulence environment. The analysis is grounded on the usual exact expressions for the various characteristic displacements and consumption speeds, widely used in turbulent combustion modeling. Prior to this analysis, the validity of the implication on these characteristic speeds of the thin flamelet framework, introduced to perform the derivation of the relation between the turbulent flame brush dynamics and the turbulent burning velocity, is evaluated from direct numerical simulation (DNS) of a turbulent premixed jet-flame.

Keywords: Turbulent premixed flames, Turbulent burning velocity, Turbulent flame brush, Bi-Modal-Limit theory

*Corresponding author

Email address: luc.vervisch@insa-rouen.fr (Luc Vervisch)

Nomenclature

$\overline{c}$	Reynolds averaged progress variable
$\tilde{c}$	Favre averaged progress variable
$V_r(c)$	Displacement speed of the iso-c surface
S_c	Consumption speed of a laminar reaction zone
S_L^o	Laminar burning velocity
$\overline{V}_T(\overline{c})$	Displacement speed of the iso-$\overline{c}$ surface
$\widetilde{V}_T(\tilde{c})$	Displacement speed of the iso-$\tilde{c}$ surface
$\tilde{S}_c$	Consumption speed of the turbulent flame brush
S_T	Turbulent burning velocity
δ_T	Turbulent flame brush thickness

1. Introduction

Back twenty years ago, Prof. Ken Bray was used to visit Normandy every year and we were lucky to enjoy endless discussions on flame physics and turbulent combustion modeling. The turbulent burning velocity was a recurrent subject, leading to notes that were left unpublished. Mainly because some of these results were quite intriguing, unfortunately without directly leading to novel modeling ideas ready for simulating flames, and all of us were, at that time, more attracted by the rapidly growing Large Eddy Simulation (LES) tools than by dealing with additional manipulations of those 'old fashion concepts'.

However, in turbulent reacting flow physics there is no getting away from certain facts and the vast literature on the subject (see [1–20] and multiple references therein), suggests that the turbulent burning velocity is one of them. How it relates to global turbulence and flame properties still motivates combustion scientists, bringing new ideas and novel challenges for real combustion systems. Thereby observations resulting from simple manipulations of the balance equation for a progress variable may still be of interest.

One of the things appearing when generalising to a turbulent flame brush the basic concepts of displacement and consumption speeds, well defined and widely used to address

laminar premixed flames dynamics [2, 21–23], is the striking fact that the flame wrinkling factor (or the ratio between turbulent and laminar flame surfaces) should not be considered, and therefore modeled, independently to the scalar transport by velocity fluctuations. A constraint which may not be that easy to meet in Reynolds Average Navier Stokes (RANS) or LES of turbulent premixed flames.

Along similar lines, a relation between the turbulent burning velocity and the rate of growth of the flame brush thickness may be established. This relation is also extended to the turbulent displacement speed inside the turbulent flame brush. To the authors' knowledge, the link between these quantities has not been discussed so far under this form and it can help understanding the departure between the flame surface amplification by turbulence and the increase of the turbulent burning velocity sometimes reported, see for instance recent findings in [18].

This paper is organised as follows, fundamentals on displacement and consumption speeds are first summarised for laminar and turbulent flows, using both Reynolds and density weighted (Favre) averaging. Then, these quantities are extracted from a turbulent premixed jet flame DNS database. After that, the thin flamelet approximation is introduced and it is examined to which extend its implication on the characteristics speeds is verified in the DNS. Finally, relations between the turbulent burning velocity, the laminar burning velocity, the flame wrinkling factor and the rate of change of the flame brush thickness are derived and discussed.

2. Displacement and consumption speeds

2.1. Laminar flow

Let us consider $c(\underline{x}, t)$ a progress variable, $c = 0$ in fresh gases and $c = 1$ in fully burnt products, defined under the assumption of unity Schmidt and Lewis numbers [24]. The flow velocity vector is $\mathbf{u}$ and $V_r(c)$ is the iso-c displacement speed, namely the propagation speed relative to the flow in the normal direction $\mathbf{n} = -\nabla c/|\nabla c|$ to the iso-c surface, thus the

added velocity which allows $c(\underline{x}, t)$ to remain constant:

$$\frac{\partial c}{\partial t} + (\mathbf{u} + V_r \mathbf{n}) \cdot \nabla c = 0 \,, \tag{1}$$

so that $\mathbf{u}_{\text{abs}} = \mathbf{u} + V_r \mathbf{n}$ is the absolute velocity of the iso-c surface in the laboratory frame.

For a mass diffusive flux expressed as $-\rho D \nabla c$ where ρ is the density following the continuity equation $(\partial \rho / \partial t) + \nabla \cdot (\rho \mathbf{u}) = 0$, D a diffusive coefficient, and a burning rate $\dot{\omega}_c$, the $c-$budget may also be written

$$\frac{\partial \rho c}{\partial t} + \nabla \cdot (\rho \mathbf{u} c) = \nabla \cdot (\rho D \nabla c) + \dot{\omega}_c = -\rho V_r \mathbf{n} \cdot \nabla c = \rho V_r |\nabla c| \,, \tag{2}$$

and

$$V_r = \frac{\nabla \cdot (\rho D \nabla c) + \dot{\omega}_c}{\rho |\nabla c|} \,. \tag{3}$$

The consumption speed of the flame S_c is defined by an integration across the reaction zone along a direction normal to the iso-c surfaces

$$\rho_o S_c = \int_{-\infty}^{+\infty} \dot{\omega}_c d\mathbf{n} \,. \tag{4}$$

In a steady, planar and unstrained one-dimensional premixed flame, mass conservation brings the relation between S_L^o, the laminar flame speed, the consumption speed and the relative progression velocity at the fresh gases leading edge $S_L^o = S_c = V_r(c = 0)$ and also the relation with the displacement speed for all values of the progress variable

$$\rho_o S_c = \rho_o S_L^o = \rho(c) V_r(c) \,. \tag{5}$$

2.2. Turbulent flow

With $\overline{\cdot}$ denoting RANS averaging or LES filtering and $\widetilde{\cdot} = \overline{\rho \cdot} / \overline{\rho}$ the density weighted (Favre) counterpart, the following is obtained from above relations for either Reynolds av-

eraging

$$\frac{\partial \overline{c}}{\partial t} + \overline{\mathbf{u}} \cdot \nabla \overline{c} + T_c = \overline{\frac{1}{\rho}\left(\nabla \cdot (\rho D \nabla c) + \dot{\omega}_c\right)} = \overline{V_r |\nabla c|}\,, \tag{6}$$

with $T_c = \overline{\mathbf{u} \cdot \nabla c} - \overline{\mathbf{u}} \cdot \nabla \overline{c}$, or Favre averaging

$$\frac{\partial \overline{\rho}\tilde{c}}{\partial t} + \nabla \cdot (\overline{\rho}\tilde{\mathbf{u}}\tilde{c}) + \nabla \cdot \tau_c = \overline{\nabla \cdot (\rho D \nabla c)} + \overline{\dot{\omega}}_c = \overline{\rho V_r |\nabla c|}\,, \tag{7}$$

where $\tau_c = \overline{\rho \mathbf{u} c} - \overline{\rho}\tilde{\mathbf{u}}\tilde{c}$. Then, introducing $\overline{V}_T$ and $\widetilde{V}_T$ the mean or filtered relative progression velocities of the iso-$\overline{c}$ and iso-$\tilde{c}$ surfaces, respectively,

$$\frac{\partial \overline{c}}{\partial t} + (\overline{\mathbf{u}} + \overline{V}_T \overline{\mathbf{n}}) \cdot \nabla \overline{c} = 0\,, \tag{8}$$

$$\frac{\partial \tilde{c}}{\partial t} + (\tilde{\mathbf{u}} + \widetilde{V}_T \tilde{\mathbf{n}}) \cdot \nabla \tilde{c} = 0\,, \tag{9}$$

with $\overline{\mathbf{n}} = -\nabla \overline{\mathbf{n}}/|\nabla \overline{\mathbf{n}}|$ and $\tilde{\mathbf{n}} = -\nabla \tilde{\mathbf{n}}/|\nabla \tilde{\mathbf{n}}|$. The definition of the displacement speeds through the turbulent flame brush thus read

$$\overline{V}_T = \frac{\overline{\frac{1}{\rho}\left(\nabla \cdot (\rho D \nabla c) + \dot{\omega}_c\right)} - T_c}{|\nabla \overline{c}|} = \frac{\overline{V_r |\nabla c|} - T_c}{|\nabla \overline{c}|}\,, \tag{10}$$

$$\widetilde{V}_T = \frac{\overline{\nabla \cdot (\rho D \nabla c)} + \overline{\dot{\omega}}_c - \nabla \cdot \tau_c}{\overline{\rho}|\nabla \tilde{c}|} = \frac{\overline{\rho V_r |\nabla c|} - \nabla \cdot \tau_c}{\overline{\rho}|\nabla \tilde{c}|}\,. \tag{11}$$

According to (8) and (9), the knowledge of $\overline{V}_T(\overline{c})$ or of $\widetilde{V}_T(\tilde{c})$ at all the points within the flame brush, would provide a complete closure of the balance equation for the progress variables $\overline{c}$ or $\tilde{c}$. This constitutes the basis of widely used modeling for turbulent premixed flames in RANS context [25]. A similar conclusion is reached introducing the so-called G-Equation [26], which provides a unique framework to explore the dynamics of a turbulent flame brush, also in the LES context, see N. Peters textbook where numerous relations and modeling to simulate turbulent flames are examined along these lines [2].

Within the Reynolds averaging context, introducing the surface averaging [27, 28]

$$\langle \cdot \rangle_s = \frac{\overline{\cdot\,|\nabla c|}}{\overline{|\nabla c|}}\,, \tag{12}$$

leads to

$$\overline{V_r|\nabla c|} = \langle V_r \rangle_s \, \overline{|\nabla c|}\,, \tag{13}$$

and with $\mathbf{u}' = \mathbf{u} - \overline{\mathbf{u}}$

$$\begin{aligned} T_c = \overline{\mathbf{u}\cdot\nabla c} - \overline{\mathbf{u}}\cdot\nabla\overline{c} = -(\overline{\mathbf{u}\cdot\mathbf{n}|\nabla c|} - \overline{\mathbf{u}}\cdot\overline{\mathbf{n}|\nabla c|}) &= -\left(\langle \mathbf{u}\cdot\mathbf{n}\rangle_s - \overline{\mathbf{u}}\cdot\langle \mathbf{n}\rangle_s\right)\overline{|\nabla c|}\,, \\ &= -\langle \mathbf{u}'\cdot\mathbf{n}\rangle_s \, \overline{|\nabla c|}\,. \end{aligned} \tag{14}$$

Combining these relations with (10), $\overline{V}_T$ may be expressed in terms of the unresolved flame surface wrinkling $\Xi = \overline{|\nabla c|}/|\nabla\overline{c}|$

$$\overline{V}_T = \left[\langle V_r \rangle_s + \langle \mathbf{u}'\cdot\mathbf{n}\rangle_s\right]\Xi\,. \tag{15}$$

Where, as expected, it is seen that the surface displacement speeds of the iso-$\overline{c}$ surfaces evolve with the flame surface wrinkling. In addition, $\langle \mathbf{u}'\cdot\mathbf{n}\rangle_s$, the transport by velocity fluctuations can increase or decrease $\overline{V}_T$ relative to the contribution of $\langle V_r \rangle_s$, the conditional surface mean of the displacement speed.

3. Direct numerical simulation database

A previously developed direct numerical simulation database (DNS) of a turbulent premixed jet flame is now probed to examine the above relations for the displacement speeds and their extension to the thin flame regime. The configuration of this DNS is from the experiment reported in [29, 30], with a coflow temperature imposed at the adiabatic burnt gases temperature.

This DNS database was explored in [31] to study the local volumetric dilatation rate

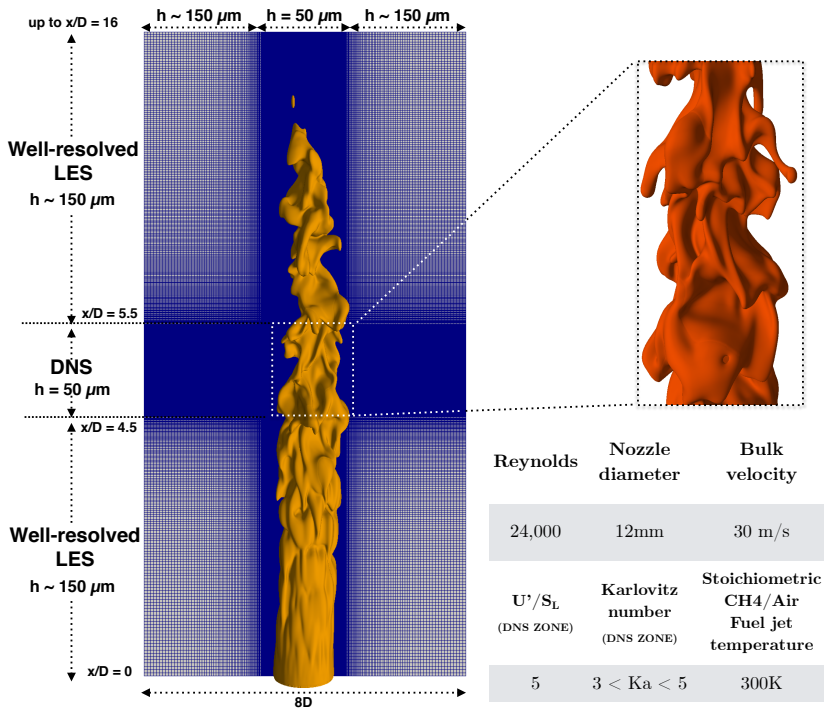

Reynolds	Nozzle diameter	Bulk velocity	Kinetic energy
24,000	12mm	30 m/s	3.82 m²/s²
U'/S_L (DNS ZONE)	Karlovitz number (DNS ZONE)	Stoichiometric CH4/Air Fuel jet temperature	Burnt gases pilot temperature
5	$3 < \mathrm{Ka} < 5$	300K	2200K

Figure 1: Three LES-DNS zones of the jet-flame simulation. Mesh and iso-progress variable $c = 0.8$. h denotes the mesh resolution.

and progress variable field characteristic geometries and also in [32] to investigate the effects of the local flow topologies upon the structure of the premixed turbulent flame. The same database served to investigate one-dimensional filtered flame sub-grid scale modeling in the light of an approximate deconvolution operation [33]. In this former work, it was discussed how the strongly convoluted three-dimensional turbulent flame surface leads to significant departure from the one-dimensional flamelet response. This DNS provided also in [34] the basis to discuss direct mapping from LES resolved scales to filtered-flame generated manifolds using convolutional neural networks (CNN).

The detail on the generation of this DNS and its main features may be found in [33] and are not repeated here for brevity, the main properties are summarised in Fig 1. This simulation relies on the idea that a well-resolved LES of the close field of a turbulent premixed and piloted jet-flame generates a flow which can be used as the inlet plane of a DNS of the interaction between velocity fluctuations and a premixed reaction zone. The LES and the

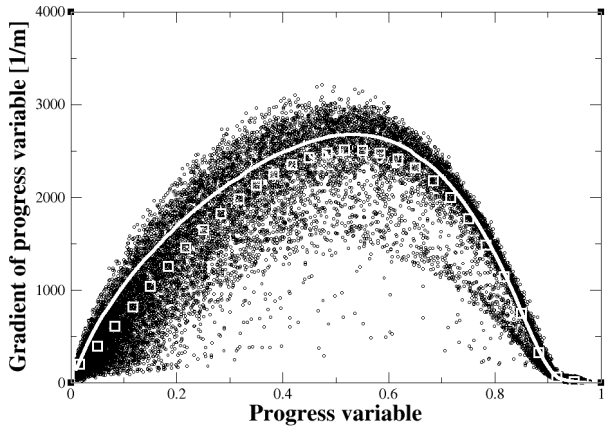

Figure 2: Magnitude of the gradient of the progress variable. Scatter plot: $|\nabla c|$ DNS (0.5% of the points shown); Square: $\left(\overline{|\nabla c| \mid c^*}\right)$; Solid line: $G(c) = |\nabla c|$ 1D-flamelet.

DNS are run simultaneously and this is achieved by embedding, inside the LES mesh, a zone where the resolution is sufficiently high so as to resolve the thin reaction zone and the Kolmogorov scale (Fig 1). The smallest scales missing in the upstream LES part rapidly cascade in the DNS zone and the fully resolved flame interacts with a turbulence which is, hopefully, more realistic that any synthetic velocity fluctuations, also including the largest scales and the mean shears, which are resolved from the inlet. The total number of mesh cells is 171 million for the LES parts and 28.58 million for the imbedded DNS zone with mesh resolutions of 150 μm (LES) and 50μm (DNS), respectively (Fig 1).

Premixed flame detailed tabulated chemistry is built with unity Schmidt numbers from the GRI-3.0 [35] methane-air mechanism with the progress variable defined form major products (CO, CO_2, H_2O) and NOx [36], in order to better reproduce the relaxation towards equilibrium fully burnt products featuring large chemical time scales. The LES part is simulated with a progress variable presumed probability density function (pdf) approach [37] and the sub-grid scale (SGS) momentum fluxes are approximated with the Vreman model [38]. The flow solver SiTCom [39] was used which considers the aerothermochemistry equations in their fully compressible form together with the balance equation for the filtered progress variable. The convective terms are discretised with a fourth-order centered skew-symmetric-like

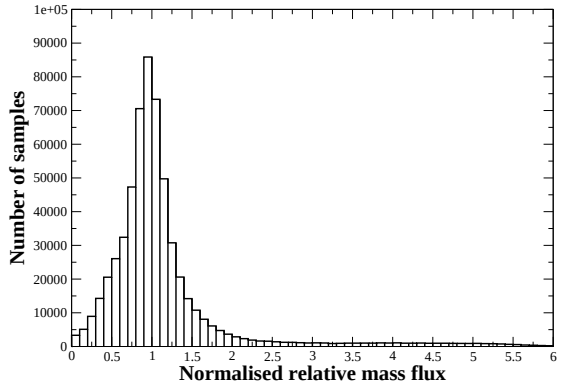

Figure 3: Histogram of $\rho V_r/(\rho_o S_L^o)$ from Eq. (3).

scheme [40] and the diffusive terms with a fourth-order centered scheme. Time is advanced explicitly with a third order Runge-Kutta method and acoustic boundary conditions [41] are imposed at inlet and outlet, with the measured profiles with synthetic turbulence [42] prescribed at inlet.

Various quantities are extracted from this DNS database, with or without formulating the thin-flamelet approximation introduced in the next section. In a preliminary analysis, the distribution of $|\nabla c|$, the magnitude of the gradient of the progress variable, is given in Fig. 2. The scatter plot within the DNS zone of $|\nabla c|$ versus the progress variable shows quite large variations within the flame. However, over the reaction zone (i.e., $0.8 < c < 0.9$), the conditional mean $\left(\overline{|\nabla c| \mid c^*}\right)$ (squares in Fig. 2) becomes close to $G(c)$ (solid line), the gradient as observed in the one-dimensional laminar flame which served for tabulating the chemistry. Because of the specific progress variable used which was originally designed to also capture also slow NOx chemistry [36], c is slowly evolving towards unity in the burnt gases and $G(c)$ almost vanishes well before $c \to 1$. In the fresh gases and in the preheating zone, the turbulence impacts on the flame structure and $\left(\overline{|\nabla c| \mid c^*}\right)$ becomes smaller than $G(c)$.

The histogram of the displacement speed ρV_r computed from Eq. (3) and normalised

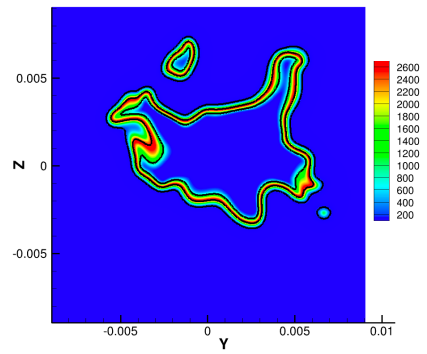

(a) $|\nabla c|$

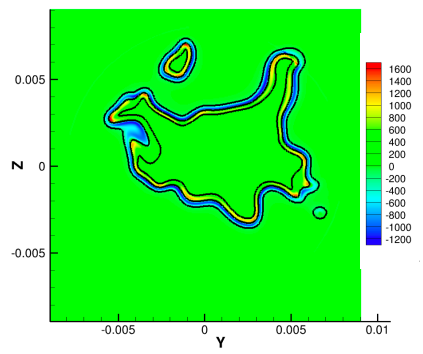

(b) $\nabla \cdot (\rho D \nabla c)$

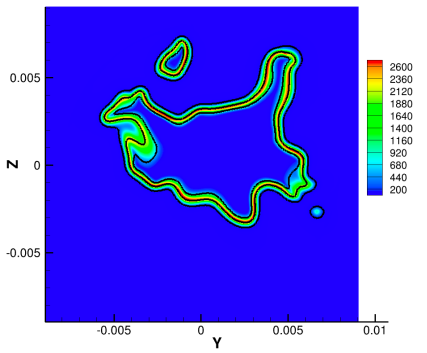

(c) $\dot{\omega}_c$

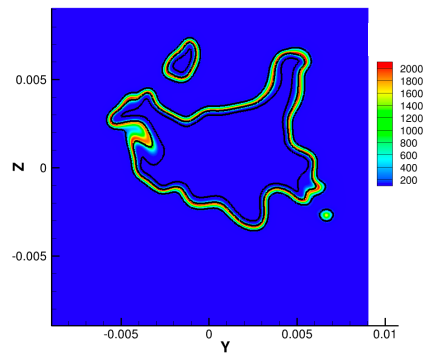

(d) $G(c)$

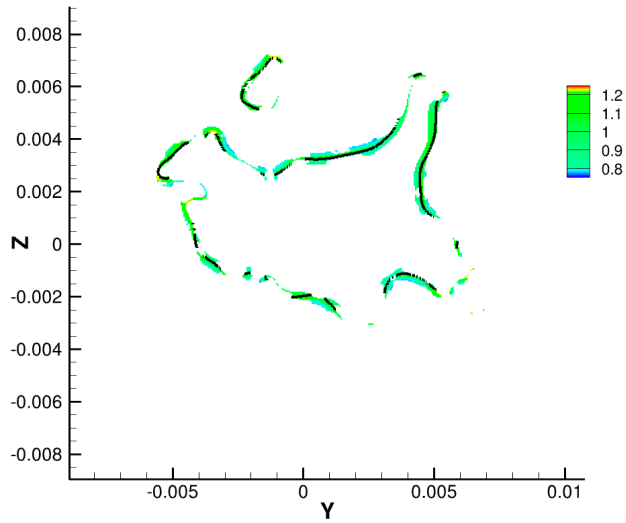

(e) $\rho V_r/(\rho_o S_L^o)$ where $|\nabla c| = (1 \pm 5\%)G(c)$

Figure 4: (a)-(c): various terms contributing to V_r (Eq. (3)); Gradients in m^{-1}. Source term in $\mathrm{kg} \cdot \mathrm{m}^{-3} \cdot \mathrm{s}^{-1}$. (d): $G(c)$ gradient mapped from 1D reference flamelet. (e): Normalised relative progression velocity at flamelet-like locations (lenghts in m).

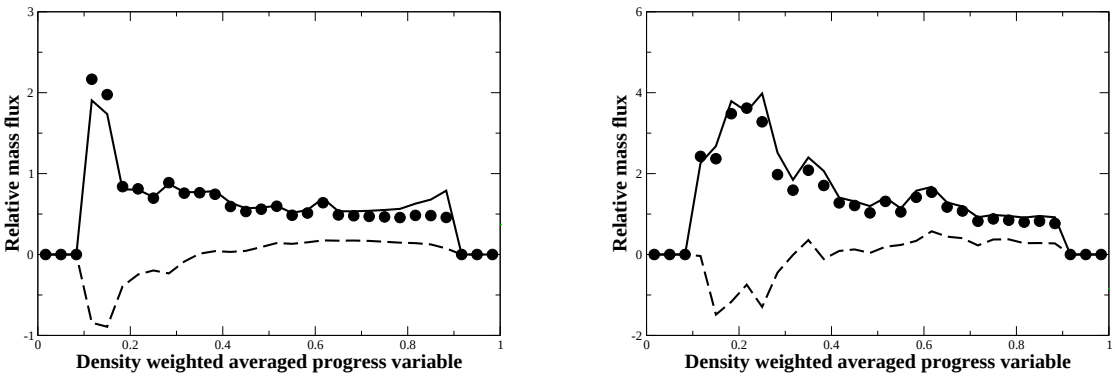

(a) All points

(b) $|\nabla c| = (1 \pm 5\%)G(c)$

Figure 5: $\left\langle \overline{\rho}\widetilde{V}_T|\tilde{c}\right\rangle$. Solid line: Eq. (11). Circle: Thin flamelet approximation (Eq. (16)). Dashed line: Scalar turbulent transport $\langle \nabla \cdot \tau_c|\tilde{c}\rangle$.

by $\rho_o S_L$ is given in Fig. 3. Even though a non-flamelet behavior was seen in the gradient plots, the statistics of V_r stays well centred around the flamelet response (Eq. (5)). This is understood from Fig. 4, where snapshots of the various terms contributing to V_r are displayed. Comparing Fig. 4(a) with Fig. 4(d) shows that the departure of $|\nabla c|$ from the one-dimensional flamelet gradient $G(c)$, occurs in zones where the flame surface is highly curved, with a pronounced thickening of the progress variable profiles.

This database built in the configuration of a real jet-flame thus combines typical flamelet and non-flamelet responses, which is expected for the Karlovitz numbers considered (Fig. 1).

4. Thin flamelet approximation and BML analysis

To introduce the turbulent burning velocity, which relates to an averaged mass burning rate, it is necessary to incorporate the density in the formulation and therefore to focus on Favre averaging or filtering. Because the flame wrinkling $\Xi = \overline{|\nabla c|}/|\nabla \overline{c}|$ is defined from Reynolds averaging, an explicity relation between $\overline{c}$ and $\tilde{c}$ must also be used, such relation is readily available introducing the Bray Moss Libby (BML) theory in the analysis [24, 43].

4.1. Thin flamelet approximation

Introducing the thin flamelet approximation (Eq. (5)) into the Favre averaging expression (10) leads to

$$\overline{\rho}\widetilde{V}_T = \rho_o S_L^o \frac{\overline{|\nabla c|}}{|\nabla \tilde{c}|} - \frac{\nabla \cdot \tau_c}{|\nabla \tilde{c}|} \,. \tag{16}$$

Figures 5 show $\overline{\rho}\widetilde{V}_T$ computed from Eq. 11 in the jet-flame DNS. The averaging procedure is done over vertical lines (streamwise direction) as in [18], here to get 343×343 distributions of $\overline{\rho}\widetilde{V}_T$ and $\tilde{c}$ from averaging over the 243 points of the vertical direction. Then $\left\langle \overline{\rho}\widetilde{V}_T | \tilde{c} \right\rangle$, the conditional mean versus the density weighted progress variable, is calculated over the 117649 averaged values to visualise the mean response through the flame brush. The circles in these plots are the values obtained from the thin flamelet approximation (RHS of (16)). A good agreement is found between $\overline{\rho}\tilde{V}_T$ from (11) and its thin flame expression (16). The contribution of $\nabla \cdot \tau_c$, the divergence of the transport by unresolved velocity fluctuation (dashed line in Fig. 5), is far from being negligible and approximating $\overline{\rho}\widetilde{V}_T$ without it would lead to error in the estimation of the relative progression velocity of the iso-$\tilde{c}$. Selecting only the points where the local reaction zone features a progress variable gradient close to $G(c)$, the 1D-flamelet one, (i.e., $|\nabla c| = (1 \pm 5\%)G(c)$), as expected the agreement gets better between the exact expression of $\overline{\rho}\widetilde{V}_T$ and its flamelet approximation.

The same is done within LES context, filtering the DNS with Gaussian filters of characteristic sizes $\Delta = 0.6\text{mm} = 1.5\delta_L$ and $\Delta = 1.200\text{mm} = 3\delta_L$, leading to the results presented in Fig. 6 (28.58 million of filtered values used for conditional averaging). With space filtering, the agreement between $\overline{\rho}\tilde{V}_T$ and its thin flame expression is also greater when conditioning on the flamelet-like points (Figs 6(c) and 6(d)).

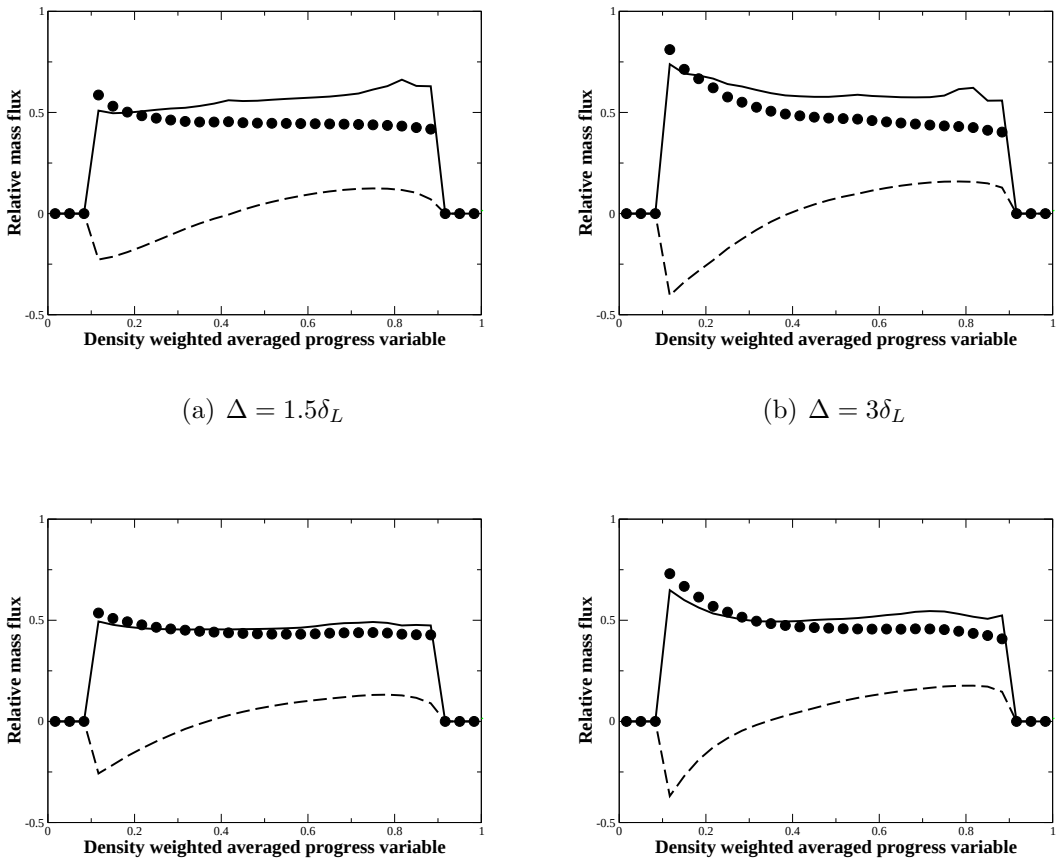

(a) $\Delta = 1.5\delta_L$

(b) $\Delta = 3\delta_L$

(c) $\Delta = 1.5\delta_L$ and $|\nabla c| = (1 \pm 5\%)G(c)$

(d) $\Delta = 3\delta_L$ and $|\nabla c| = (1 \pm 5\%)G(c)$

Figure 6: $\left\langle \overline{\rho}\widetilde{V}_T|\tilde{c}\right\rangle$. LES filtering ($\Delta$ = 600 and 1200 µm). (a)-(b) all DNS points. (c)-(d): only points featuring 1D flamelet gradient. Solid line: Eq. (11). Circle: Thin flamelet approximation (Eq. (16)). Dashed line: Scalar sub-grid turbulent transport $\langle \nabla \cdot \tau_c|\tilde{c}\rangle$.

4.2. Bi-Modal-Limit analysis

Within the context of the strict bi-modal-limit (BML) theory [24, 43], the probability density function (PDF) of the progress variable reads

$$\overline{P}(c^*) = \alpha\delta(c^*) + \beta\delta(1 - c^*) \,. \tag{17}$$

PDF normalisation implies $\alpha + \beta = 1$ and

$$\overline{c} \;=\; \int_0^1 c^* \overline{P}(c^*) dc^* = \beta \,, \tag{18}$$

$$\overline{\rho}\tilde{c} \;=\; \overline{\rho c} = \int_0^1 \rho(c^*) c^* \overline{P}(c^*) dc^* = \rho_b \beta \,, \tag{19}$$

therefore $\beta = \overline{c} = \overline{\rho}\tilde{c}/\rho_b$. Then,

$$\overline{\rho} = \int_0^1 \rho(c^*)\overline{P}(c^*)dc^* = \left(1 - \frac{\overline{\rho}\tilde{c}}{\rho_b}\right)\rho_o + \frac{\overline{\rho}\tilde{c}}{\rho_b}\rho_b = \rho_o + \overline{\rho}\tilde{c}(1 - \rho_o/\rho_b) = \rho_o - \overline{\rho}\tau\tilde{c} \,, \tag{20}$$

with $\tau = (\rho_o/\rho_b) - 1 = (T_b/T_o) - 1$. From (20) $\overline{\rho} = \rho_o/(1 + \tau\tilde{c})$ and $\overline{c} = \overline{\rho}\tilde{c}/\rho_b$, the relation between $\overline{c}$ and $\tilde{c}$ is obtained:

$$\overline{c} = \frac{(1 + \tau)\tilde{c}}{1 + \tau\tilde{c}} \,, \tag{21}$$

also,

$$|\nabla\tilde{c}| = \left(\frac{\rho_o}{\overline{\rho}}\right)^2 \frac{1}{1 + \tau}|\nabla\overline{c}| \,, \tag{22}$$

and Eq. (16) becomes

$$\overline{\rho}\widetilde{V}_T = (1 + \tau)\left(\frac{\overline{\rho}}{\rho_o}\right)^2 \rho_o S_L^o \Xi - \frac{\nabla \cdot \tau_c}{|\nabla\tilde{c}|} \,. \tag{23}$$

In the particular case of a steady and planar turbulent flame brush, from mass conservation the turbulent burning velocity S_T is defined so that

$$\overline{\rho}\widetilde{V}_T = \rho_o S_T \, . \tag{24}$$

Therefore the product $\overline{\rho}(\tilde{c})\widetilde{V}_T(\tilde{c})$ should not depend on $\tilde{c}$ and from the relation (23), the flame wrinkling, Ξ, and the transport by unresolved velocity fluctuations $\nabla \cdot \tau_c$ should not, in theory, be modelled independently of each other to secure this weak dependence on $\tilde{c}$.

The fact that the product $\overline{\rho}(\tilde{c})\widetilde{V}_T(\tilde{c})$ should not depend much on $\tilde{c}$ cannot strickly be verified in the post-processing of the DNS considered in this study, since it includes finite-rate chemistry and therefore cannot exhibit the asymptotic bi-modal behavior. However, Figs. 5 and 6 show that $\overline{\rho}(\tilde{c})\widetilde{V}_T(\tilde{c})$ weakly varies over a quite large range of variation of $\tilde{c}$. Therefore, it appears that the implications of the bi-modal analysis on the statistical behavior of the flame are in fact more robust than expected. Accordingly, it makes sense to adopt the above BML formalism to pursue the analysis towards the dynamics of the flame brush thickness.

4.3. Flame surface in the Bi-Modal-Limit

The surface density function $\Sigma(c^*) = \left(\overline{|\nabla c||c^*}\right)\overline{P}(c^*)$ is introduced [44–46] so that

$$\overline{|\nabla c|} = \Xi|\nabla \overline{c}| = \int_0^1 \Sigma(c^*)dc^* = \int_0^1 \left(\overline{|\nabla c||c^*}\right)\overline{P}(c^*)dc^* \, , \tag{25}$$

where $\left(\overline{\cdot\,|c^*}\right)$ denotes a conditional average. The turbulent consumption speed $\tilde{S}_c$ may then be written

$$\rho_o \tilde{S}_c = \int_{-\infty}^{+\infty} \overline{\dot{\omega}}_c d\xi = \int_0^1 \left[\int_0^1 \dot{\omega}_c \overline{P}(c^*) dc^* \right] \frac{d\overline{c}}{|\nabla \overline{c}|} , \tag{26}$$

$$= \int_0^1 \left[\int_0^1 \dot{\omega}_c \frac{\Sigma(c^*)}{\left(\overline{|\nabla c||c^*}\right)} dc^* \right] \frac{d\overline{c}}{|\nabla \overline{c}|} , \tag{27}$$

where ξ denotes the coordinate in the direction normal to the reaction zone, assuming that the iso-scalar surfaces are quasi-parallel. In the thin reaction zone limit, $\Sigma(c^*) \approx \overline{|\nabla c|}$ and $\left(\overline{|\nabla c||c^*}\right) \approx dc^*/d\xi \ \forall c^*$, then (27) becomes

$$\rho_o \tilde{S}_c = \int_0^1 \overline{|\nabla c|} \left[\int_0^1 \dot{\omega}_c \frac{dc^*}{\left(\overline{|\nabla c||c^*}\right)} \right] \frac{d\overline{c}}{|\nabla \overline{c}|} = \int_0^1 \Xi \left[\int_{-\infty}^{+\infty} \dot{\omega}_c d\xi \right] d\overline{c} = \rho_o S_L^o \Xi , \tag{28}$$

where Eqs. (4) and (5) have been used and where it is also assumed that Ξ weakly varies with $\overline{c}$. This last relation (Eq. (28)) which directly relates the turbulent consumption speed to the flame wrinkling will be useful to explicitly introduce the turbulent flame brush thickness in the analysis.

5. Scaling of turbulent burning velocity with flame brush thickness variation rate

To relate the flame brush thickness and the displacement speeds, the mass conservation and the progress variable equation (Eq. (7)) may be integrated through the turbulent reaction zones.

Still denoting ξ the coordinate in the direction normal to the reaction zone ($d\xi = d\overline{c}/|\nabla \overline{c}|$)

and with the boundary condition $\tilde{c}=0$, $\rho=\rho_o$ for $\xi\to-\infty$ and $\tilde{c}=1$ for $\xi\to+\infty$,

$$\frac{\partial}{\partial t}\int_{-\infty}^{+\infty}\overline{\rho}d\xi+(\overline{\rho}\tilde{\mathbf{u}})_{+\infty} = (\overline{\rho}\tilde{\mathbf{u}})_{-\infty}=\rho_o S_T\,, \tag{29}$$

$$\frac{\partial}{\partial t}\int_{-\infty}^{+\infty}\overline{\rho}\tilde{c}d\xi+(\overline{\rho}\tilde{\mathbf{u}})_{\infty} = \int_{-\infty}^{+\infty}\overline{\dot{\omega}}_c d\xi=\rho_o\tilde{S}_c\,. \tag{30}$$

From these relations

$$S_T-\tilde{S}_c=\frac{\partial}{\partial t}\int_{-\infty}^{+\infty}\frac{\overline{\rho}}{\rho_o}\left(1-\tilde{c}\right)d\xi\,. \tag{31}$$

Let us change variable introducing $\eta(t)=\xi/\delta_T(t)$, where $\delta_T(t)$ is the mean flame brush thickness. Then, for every variable $\phi(\xi,t)=\phi(\eta(t))$

$$\begin{aligned}\frac{\partial}{\partial t}\int_{\xi_1}^{\xi_2}\phi(\xi,t)d\xi &= \int_{\eta_1}^{\eta_2}\frac{d\phi(\eta)}{d\eta}\frac{d\eta}{dt}\delta_T(t)d\eta=\int_{\eta_1}^{\eta_2}\frac{d\phi(\eta)}{d\eta}\left(-\frac{\eta}{\delta_T(t)}\frac{d\delta_T(t)}{dt}\right)\delta_T(t)d\eta\,,\\ &= -\frac{d\delta_T(t)}{dt}\int_{\eta_1}^{\eta_2}\frac{d\phi}{d\eta}\eta d\eta=-\frac{d\delta_T(t)}{dt}\left([\phi\eta]_{\eta_1}^{\eta_2}-\int_{\eta_1}^{\eta_2}\phi d\eta\right)\,.\end{aligned} \tag{32}$$

Applied to the integral term in (31) this relation returns

$$\frac{\partial}{\partial t}\int_{-\infty}^{+\infty}\frac{\overline{\rho}}{\rho_o}\left(1-\tilde{c}\right)d\xi=\frac{d\delta_T(t)}{dt}\underbrace{\int_{\eta_-}^{\eta_+}\frac{\overline{\rho}(\eta)}{\rho_o}\left(1-\tilde{c}(\eta)\right)d\eta}_{\mathcal{I}_1>0}\,, \tag{33}$$

where $\eta^{\pm}$ ($\eta^-\approx 0$ and $\eta^+\approx 1$) denote the cold and hot edges of the mean flame brush. The relation (31) with (33) and (28) becomes

$$S_T=\tilde{S}_c+\mathcal{I}_1\frac{d\delta_T}{dt}=S_L^o\Xi+\mathcal{I}_1\frac{d\delta_T(t)}{dt}\,. \tag{34}$$

Therefore, even under the hypothesis of thin and unstrained premixed flamelets, the turbulent flame speed can loose its direct linear proportionality to the flame area, as the flame brush thickness increases or decreases (i.e., for $d\delta_T(t)/dt \neq 0$).

A governing equation for the flame brush thickness $\delta_T(t)$ has been discussed from first principles [2, 47, 48] leading to a scaling law for its relaxation starting from an initial condition $\delta_T(t_o)$ within a turbulence featuring ℓ_T and τ_T as turbulent integral length and time scales, respectively,

$$\delta_T^2(t) = b_1^2 \ell_T^2 \left(1 - \exp(-b_2(t - t_o)/\tau_T)\right) + \delta_T^2(t_o) \exp(-b_2(t - t_o)/\tau_T) \,, \tag{35}$$

where b_1 and b_2 are two parameters determined by expected asymptotic behaviors [2] or DNS [48]. The relation (35) suggests a relaxation of the turbulent flame brush thickness following an exponential behaviour towards a value proportional to ℓ_T. The time variation of $\delta_T(t)$ is therefore controlled by the distribution of ℓ_T and τ_T encountered by the reaction zones, with $d\delta_T(t)/dt$ rapidly evolving for the short time-scales ($t - t_o < \tau_T$), when the flame brush thickness is submitted to a non-uniform turbulence environment.

According to Eq. (34) this can lead to a quite large variety of responses of S_T versus the integral turbulent length scale, depending on whether it is driven mainly by $S_L^o \Xi$ or by $\mathcal{I}_1 d\delta_T(t)/dt$, or again by an equilibrium between both of them.

We cannot investigate in detail this specific point from the DNS discussed above because it is limited to a streamwise length of one burner diameter, hence with an almost uniform δ_T over the DNS zone. In fact most standard DNS suffers from such limitation. However, the link between ℓ_T and S_T was recently thoroughly discussed in [18] to conclude that S_T can increase exponentially with the integral scale, for ℓ_T up to about 6 laminar flame thicknesses, evolution followed by a power-law scaling for larger values of ℓ_T. This was observed together with S_T loosing its proportionality to the flame surface area as the integral length scale increases, as expected from (34) combined with (35).

The very same analysis can be pursued in a frame moving with the mean flame brush

and by integrating the continuity equation from the cold edge of the flame up to a point $\eta^\star = \xi^\star/\delta_T(t)$ located between fresh and burnt gases:

$$\frac{\partial}{\partial t}\int_{-\infty}^{\xi^\star} \overline{\rho} d\xi + \overline{\rho}\widetilde{V}_T(\xi^\star) = \rho_o S_T \,, \tag{36}$$

$$\rho_o \frac{d\delta_T(t)}{dt} \underbrace{\int_{\eta^-}^{\eta^\star} -\eta \left(\frac{d(\overline{\rho}/\rho_o)}{d\eta}\right) d\eta}_{\mathcal{I}_2(\eta^\star)>0} + \overline{\rho}\widetilde{V}_T(\eta^\star) = \rho_o S_T \,. \tag{37}$$

Combined with Eq. (34) and using the fact that through the turbulent flame $\eta = \eta(\tilde{c})$,

$$\overline{\rho}(\tilde{c})\widetilde{V}_T(\tilde{c}) = \rho_o S_L^o \Xi + \rho_o(\mathcal{I}_1 - \mathcal{I}_2(\tilde{c}))\frac{d\delta_T(t)}{dt} \,. \tag{38}$$

Where for $\tilde{c} \to 0$, $\mathcal{I}_2(\tilde{c}) \to 0$ and the cold leading edge relation $\rho_o S_T = \overline{\rho}_o \widetilde{V}_T(\tilde{c} \to 0)$ is recovered. Equation (38) reveals that, within the turbulent flame brush, the displacement speeds of the iso-$\tilde{c}$ surfaces are not simply proportional to the leading edge turbulent flame speed, but varies according to the dynamics of the flame brush thickness itself. Which according to (35) directly relates to the local turbulence properties and specifically to their eventual relaxation with time, making the modeling of S_T from global turbulence quantities quite challenging.

Finally, the combination of (23) with (38) illustrates the intricate links between turbulent transport, flame wrinkling and the variation of the flame brush thickness.

$$\nabla \cdot \tau_c = \rho_o |\nabla \tilde{c}| \left(\left[(1+\tau)\left(\frac{\overline{\rho}}{\rho_o}\right)^2 - 1 \right] S_L^o \Xi - (\mathcal{I}_1 - \mathcal{I}_2(\tilde{c}))\frac{d\delta_T(t)}{dt} \right) \,. \tag{39}$$

This last relation goes along with the well-known dependence of the gradient or counter gradient behaviors of the scalar turbulent transport on the dynamics of the turbulent flame brush thickness [49, 50].

6. Conclusion

A relation between the variation rate of the turbulent flame brush thickness, the flame wrinkling and the turbulent burning velocity is established from the progress variable balance equation combined with the Bray-Moss-Libby (BML) theory. This relation derives from exact expressions for the relative progression velocities widely used in premixed turbulent flame analysis, combined with a flamelet approximation. From direct numerical simulation (DNS), it is shown that this essentiel ingredient of the derivation (i.e., the implication of the thin hypothesis on the statistics) stays valid, even when quite strong departures from the flamelet behavior are observed locally.

The role of the time derivative of the turbulent flame brush thickness in the expression for the turbulent burning velocity may explain previously reported deviation from the direct scaling between the flame surface amplification by turbulence, the integral properties of the turbulence (integral length and time scales) and the overall burning velocity. It is also discussed how the dynamics is likely to be driven by a short time scale, which is representative of the relaxation of the turbulent flame brush towards the integral length scale. Because of the large variability in the time evolution of the turbulence properties, this suggests in return the possibility of a large range of scalings for the turbulent burning velocity.

The development in a near future of DNS databases featuring premixed turbulent flames developing in shear flows over sufficiently large distances and at Reynolds number large enough, should allow for further investigating the obtained relations.

Acknowledgments

The authors thanks Prof. Ken Bray and Shirley Bray for 30 years of warm friendship. The authors benefited from multiple fruitful collaborations with Prof. Ken Bray on reacting flow physics, including those discussed in this article.

References

[1] D. Bradley, A. K. C. Lau, M. Lawes, Flame stretch rate as a determinant of turbulent burning velocity, Phil. Trans. R. Soc. Lond. A 338 (1992) 359–387.

[2] N. Peters, Turbulent Combustion, Cambridge University Press, 2000.

[3] R. Borghi, Turbulent premixed combustion: Further discussions on the scales of fluctuations, Combust. Flame 80 (3/4) (1990) 304–312.

[4] C. Corvellec, P. Bruel, V. A. Sabel'Nikov, Turbulent premixed flames in the flamelet regime: burning velocity spectral properties in the presence of countergradient diffusion, Combustion and Flame 120 (4) (2000) 585–588.

[5] F. Charlette, C. Meneveau, D. Veynante, A power-law flame wrinkling model for LES of premixed turbulent combustion Part I: non-dynamic formulation, Combust. Flame 131 (1-2) (2002) 159–180.

[6] F. Charlette, C. Meneveau, D. Veynante, A power-law flame wrinkling model for LES of premixed turbulent combustion Part II: dynamic formulation, Combust. Flame 131 (1-2) (2002) 181–197.

[7] D. Bradley, M. Lawes, M. S. Mansour, Correlation of turbulent burning velocities of ethanol-air, measured in a fan-stirred bomb up to 1.2MPa, Combustion and Flame 158 (1) (2011) 123–138.

[8] A. R. Hawkes, O. Chatakonda, H. Kolla, A. R. Kerstein, J. H. Chen, A petascale direct numerical simulation study of the modelling of flame wrinkling for large-eddy simulations in intense turbulence, Combust Flame 159 (8) (2012) 2690–2703.

[9] M. Z. Haq, C. G. W. Shepparda, R. Woolleya, D. A. Greenhalghb, R. D. Lockettb, Wrinkling and curvature of laminar and turbulent premixed flames, Combust. Flame 131 (1-2) (2002) 1–15.

[10] O. Colin, F. Ducros, D. Veynante, T. Poinsot, A thickened flame model for Large Eddy Simulations of turbulent premixed combustion, Physics of Fluids 12 (7) (2000) 1843–1863.

[11] P. Tamadonfar, Ã. L. Gülder, Flame brush characteristics and burning velocities of premixed turbulent methane/air Bunsen flames, Combustion and Flame 161 (12) (2014) 3154–3165.

[12] S. Verma, A. N. Lipatnikov, Does sensitivity of measured scaling exponents for turbulent burning velocity to flame configuration prove lack of generality of notion of turbulent burning velocity?, Combustion and Flame 173 (2016) 77–88.

[13] K. Bray, M. Champion, P. Libby, The interaction between turbulence and chemistry in premixed turbulent flames, in: R. Borghi, S. Murphy (Eds.), Turbulent Reacting Flows, Vol. 40 of Lecture Notes in Engineering, Springer, 1989, pp. 541 – 563.

[14] K. N. C. Bray, M. Champion, P. A. Libby, N. Swaminathan, Finite rate chemistry and presumed PDF models for premixed turbulent combustion, Combust. Flame 146 (4) (2006) 665–673.

[15] R. K. Cheng, T. T. Ng, On defining the turbulent burning velocity in premixed V-shaped turbulent flames, Combustion and Flame 57 (2) (1984) 155–167.

[16] K. N. C. Bray, M. Champion, P. A. Libby, Pre-mixed flames in stagnating turbulence: Part Vevaluation of models for the chemical source termm, Combustion and Flame 127 (1) (2001) 2023–2040.

[17] E. Knudsen, H. Pitsch, A dynamic model for the turbulent burning velocity for large eddy simulation of premixed combustion, Combustion and Flame 154 (4) (2008) 740–760.

[18] A. Attili, S. Luca, D. Denker, F. Bisetti, H. Pitsch, Turbulent flame speed and reaction layer thicknening in premixed jet flames at constant Karlovitz and increasing Reynolds numbers, Proc. Combust. Inst. in press (2021) –.

[19] S. A. Filatyev, J. F. Driscoll, C. D. Carter, J. M. Donbar, Measured properties of turbulent premixed flames for model assessment, including burning velocities, stretch rates, and surface densities, Combustion and Flame 141 (1) (2005) 1–21.

[20] L. J. Jiang, S. S. Shy, W. Y. Li, H. M. Huang, M. T. Nguyen, High-temperature, high-pressure burning velocities of expanding turbulent premixed flames and their comparison with Bunsen-type flames, Combustion and Flame 172 (2016) 173–182.

[21] T. Poinsot, D. Veynante, Theoretical and Numerical Combustion, R. T. Edwards, Inc., 2005.

[22] C. K. Law, Combustion Physics, Cambridge University Press, 2006.

[23] P. Clavin, G. Searby, Combustion Waves and Fronts in Flows, Cambridge University Press, Cambridge, 2016.

[24] K. N. C. Bray, The Challenge of turbulent combustion, Symp. (Int.) on Combust. 26 (1996) 1–26.

[25] V. Zimont, Gas Premixed Combustion at High Turbulence. Turbulent Flame Closure Model Combustion Model, Experimental Thermal and Fluid Science 21 (2000) 179–186.

[26] A. R. Kerstein, W. T. Ashurst, F. Williams, Field equation for interface propagation in an unsteady homogeneous flow field, Physical Review A 33 (7) (1988) 2728.

[27] D. Veynante, L. Vervisch, Turbulent Combustion Modeling, Prog Energy Combust Sci 28 (2002) 193–266.

[28] L. Vervisch, D. Veynante, Interlinks between approaches for modeling turbulent flames, Proc. Combust. Inst. 28 (2000) 175–183.

[29] Y.-C. Chen, N. Peters, G. A. Schneemann, N. Wruck, U. Renz, M. S. Mansour, The detailed flame structure of highly stretched turbulent premixed methane-air flames, Combust. Flame 107 (3) (1996) 223–244.

[30] M. S. Mansour, Y.-C. Chen, N. Peters, Highly strained turbulent rich methane flames stabilized by hot combustion products, Combust. Flame 116 (1-2) (1999) 136–153.

[31] L. Cifuentes, C. Dopazo, J. Martin, P. Domingo, L. Vervisch, Local volumetric dilatation rate and scalar geometries in a premixed methane-air turbulent jet flame, Proc. Combust. Inst. 35 (2) (2015) 1295–1303.

[32] L. Cifuentes, C. Dopazo, J. Martin, P. Domingo, L. Vervisch, Effects of the local flow topologies upon the structure of a premixed methane-air turbulent jet flame, Flow Turbulence Combust. 96 (2) (2016) 535–546.

[33] P. Domingo, L. Vervisch, DNS and approximate deconvolution as a tool to analyse one-dimensional filtered flame sub-grid scale modeling, Combust. Flame 177 (2017) 109–122.

[34] A. Seltz, P. Domingo, L. Vervisch, Z. M. Nikolaou, Direct mapping from LES resolved scales to filtered-flame generated manifolds using convolutional neural networks, Combust. Flame 210 (2019) 71–82.

[35] G. P. Smith, D. M. Golden, M. Frenklach, N. W. Moriarty, B. Eiteneer, M. Goldenberg, C. T. Bowman, R. K. Hanson, S. Song, W. C. Gardiner, V. V. Lissianski, Z. Qin, Tech. rep., http://www.me.berkeley.edu/gri-mech/ (1999).

[36] G. Godel, P. Domingo, L. Vervisch, Tabulation of NOx chemistry for Large-Eddy Simulation of non-premixed turbulent flames, Proc. Combust. Inst. 32 (2009) 1555–1561.

[37] P. Domingo, L. Vervisch, D. Veynante, Large-Eddy Simulation of a lifted methane-air jet flame in a vitiated coflow, Combust. Flame 152 (3) (2008) 415–432.

[38] A. W. Vreman, An eddy-viscosity subgrid-scale model for turbulent shear flow: Algebraic theory and applications, Phys. Fluids. 16 (10) (2004) 3670–3681.

[39] L. Bouheraoua, P. Domingo, G. Ribert, Large-eddy simulation of a supersonic lifted jet flame: Analysis of the turbulent flame base, Combust. Flame 179 (2017) 199–218.

[40] F. Ducros, F. Laporte, T. Soulères, V. Guinot, P. Moinat, B. Caruelle, High-order fluxes for conservative skew-symmetric-like schemes in structured meshes: application to compressible flows., J. Comput. Phys. 161 (2000) 114–139.

[41] G. Lodato, P. Domingo, L. Vervisch, Three-dimensional boundary conditions for Direct and Large-Eddy Simulation of compressible viscous flows, J. Comput. Phys 227 (10) (2008) 5105–5143.

[42] M. Klein, A. Sadiki, J. Janicka, A Digital Filter Based Generation of Inflow Data for Spatially Developing Direct Numerical or Large Eddy Simulations, J. Comp. Physics 186 (2) (2002) 652–665.

[43] K. N. C. Bray, P. A. Libby, J. B. Moss, Unified modeling approach for premixed turbulent combustion – Part I: General formulation, Combustion and flame 61 (1) (1985) 87?102.

[44] S. B. Pope, The evolution of surfaces in turbulence, Int. J. Eng. Sci. 26 (5) (1988) 445–269.

[45] S. Pope, Computations of turbulent combustion: progress and challenges, in: Symp. (Int.) on Combust., Vol. 23, The Combustion Institute Pittsburgh, 1990.

[46] L. Vervisch, E. Bidaux, K. N. C. Bray, W. Kollmann, Surface density function in premixed turbulent combustion modeling, similarities between probability density function and flame surface approaches, Phys. Fluids 7 (10) (1995) 2496–2503.

[47] M. Oberlack, H. Wenzel, N. Peters, On symmetries and averaging of the G-equation for premixed turbulent combustion, Combustion Theory and Modeling 5 (2001) 363–383.

[48] H. Wenzel, N. Peters, Direct numerical simulation and modeling of kinematic restoration, dissipation and gas expansion effects of premixed flames in homogeneous turbulence, Combustion Science and Technology 158 (2000) 273–297.

[49] P. A. Libby, K. N. C. Bray, Countergradient diffusion in premixed turbulent flames, AIAA Journal 19 (2) (1981) 205.

[50] D. Veynante, A. Trouvé, K. Bray, T. Mantel, Gradient and counter-gradient scalar transport in turbulent premixed flames, J. Fluid Mech. 332 (1997) 263–293.